Couple-stresses effects on the dynamic behaviour of connecting-rod bearings in both gasoline and diesel engines

Mustapha Lahmar, Benyebka Bou-Saïd

Couple Stress Effects on the Dynamic Behavior of Connecting Rod Bearings in Both Gasoline and Diesel Engines

MUSTAPHA LAHMAR
Mechanical Engineering Department
Faculty of Science and Engineering
Guelma University
Guelma (24000), Algeria
and
BENYEBKA BOU-SAÏD (STLE Member)
Laboratoire de Mécanique des Contacts & des Solides (LaMCoS)
INSA de Lyon Bât. Jean d'Alembert
69621 Villeurbanne Cedex (F), France

An isothermal hydrodynamic analysis of big end connecting rod bearings for both diesel and gasoline engines lubricated with couple stress fluids is undertaken. Based on the V. K. Stokes micro-continuum theory, an incompressible modified Reynolds equation is derived from the fluid motion and mass conservation equations using the assumptions of thin-film theory. The hydrodynamic performance and the crank pin center trajectories are determined numerically by means of the Booker mobility technique. Compared with the Newtonian lubricant case, the lubricants with couple stresses provide an increase of the minimum film thickness, and a drastic decrease of the power loss, peak pressure, and flow rate over one engine cycle for both engines.

KEY WORDS

Couple Stress Fluids; Connecting Rod Bearing; Gasoline Engine; Diesel Engine; Mobility Method; Thin Film Theory

INTRODUCTION

The problem with the viscoelastic lubrication theory is that it mainly reduces to the determination of a realistic state constitutive equation connecting stress and the rate of deformation. It is also essential that the equation chosen be simple and mathematically permissible in the sense of invariance. Most investigations to date, while using mathematically simple models, have used either physically unrealistic or mathematically inadmissible equations of state. It thus appears that a reappraisal would be useful.

Most previous investigations have concentrated on steady-flow problems. In such situations the flow of viscoelastic liquids is indistinguishable from the flow of fluids showing non-Newtonian viscosity characteristics (referred to both as purely viscous or generalized Newtonian). The presence of nonlinearities during the simple shear flow of such a lubricant is considered to increase the load-carrying capacity of the lubricant film, whereas the reduction in the viscosity of the lubricant with shear rate contributes to the reduction in friction. The non-Newtonian behavior of the lubricant is found to delay the onset of turbulence and cavitation and to stabilize the flow.

The formulation of a single generalized constitutive equation for the investigation of different types of flow situations is almost impossible. An adequate form of the constitutive equation that can satisfactorily predict the interested aspect of the flow situation to the required accuracy is the actual requirement for an investigation. One approach used to characterize these fluids consists in considering these lubricants as polar fluids. Physically, the polar fluids consist of rigid, randomly oriented particles suspended in a viscous medium. Mineral oils containing small amounts of additives such as viscosity index (VI) improver polymers are examples that could be characterized as couple stress fluids.

The main particularity of couple stress fluids in a mathematical sense is that the stress tensor is nonsymmetric. In order to better describe the flow behavior of this kind of non-Newtonian fluid different micro-continuum theories were therefore developed (Stokes *(1)*, Ariman and Sylvester *(2)*, *(3)*). Among these theories, the couple-stress fluid model proposed firstly by V. K. Stokes *(1)* is the simplest and has been widely used. This model allows polar effects such as the presence of couple stresses and body couples in addition to the body and surface forces. Incompressible couple stress fluids are physically characterized by two constants; namely, the usual viscosity μ and a couple stress parameter η. Of course, only one parameter appears for incompressible

NOMENCLATURE

b_i	= body forces
C	= bearing radial clearance
D	= bearing diameter
e	= eccentricity
e_{ijk}	= permutation tensor
F	= applied load
F_{X_3}, F_{Y_3}	= Cartesian components of the applied load
h	= oil film thickness
$\tilde{h}$	= dimensionless film thickness
h_{min}	= minimum oil film thickness
L	= bearing length
ℓ	= characteristic length of the polymer additive
$\tilde{\ell}$	= couple stress parameter
ℓ_i^*	= body couples
ℓ_2	= crank radius
ℓ_3	= rod length
M	= mobility factor
M_e, M_ϕ	= components of the mobility vector
M_{ij}	= couple stress tensor in fluid
N	= engine speed
O_B	= bearing center
O_j	= journal center
p	= oil film pressure
$\tilde{p}$	= dimensionless pressure
P	= power loss
Q_z	= side leakage flow
R_j	= journal radius
R_b	= bearing radius
R	= bearing radius
$\Re_h$	= local Reynolds number
t	= time
u, v, w	= components of the lubricant velocity in the x, y, and z directions, respectively
$\bar{u}$, $\bar{w}$	= mean flow velocities in the x and y directions, respectively
U_j	= linear velocity of the journal surface
U_b	= linear velocity of the bearing surface
x, y, z	= local rectangular coordinates system
X_3, Y_3, Z_3	= coordinate system related to the connecting rod bearing
z	= axial coordinate
$\tilde{z}$	= dimensionless axial coordinate
α_M	= mobility direction
ε	= eccentricity ratio or scale parameter
$\dot{\varepsilon}$	= derivative of ε with respect to t
ϕ	= attitude angle
$\dot{\phi}$	= angular velocity of the line of centers
Φ	= dissipation function
ω_j	= angular velocity of journal
ω_B	= angular velocity of bearing
ω_i^*	= vorticity vector component
$\bar{\omega}$	= average angular velocity of journal and bearing relative to the load line
ψ	= angle between the direction of load and $O_B X_3$ direction
$\dot{\psi}$	= angular velocity of the applied load
θ	= bearing angle
θ_1, θ_2	= angles delimiting the cavitation zone
θ_C	= crank angle
σ_{ij}	= stress tensor
λ, μ	= dilatation and shear fluid viscosities, respectively
η, η'	= material constant responsible for the couple stress property
ρ	= lubricant density
ξ, η	= coordinate system related to the applied load
O_B, X_3, Y_3	= coordinate system relative to connecting rod

Newtonian fluids, which is the shear viscosity. In the literature, the effects of couple stresses on the behavior of journal bearings are theoretically studied by defining the dimensionless couple stress parameter $\tilde{\ell} = \frac{\ell}{C}$ where the value ranges from 0 to 1. $\ell = \sqrt{\eta/\mu}$ has the dimension of length and can be thought of as a fluid property depending on the size of the high polymer molecule.

Owing to its relative mathematical simplicity, the Stokes couple stress fluid model has been applied to analyze various hydrodynamic and hydrostatic lubrication problems. Lin *(4), (5)* investigated the effects of the couple stress parameter on the squeeze film characteristics of a long partial journal bearing and a finite length journal bearing using the Stokes micro-continuum theory. The theoretical results showed that the presence of the couple stresses provides an enhancement in the load-carrying capacity and lengthens the response time of the squeeze film action of the system as compared to the Newtonian lubricant case. It was also found that the effects of the couple stresses are more pronounced for the high values of the couple stress parameter (i.e., for a higher chain length of the additive molecule).

In another work, Lin *(6)* studied the combined effects of couple stresses, fluid inertia, and recess volume compressibility on the steady-state and dynamic performance characteristics of a hydrostatic thrust bearing. According to the results obtained, the effect of couple stresses provides an improvement in the dynamic stiffness and damping characteristics of the system and reduces the pumping power due to the decrease of the flow rate. Mokhiamer, et al. *(7)* presented an excellent theoretical study of the performance of a steadily loaded compliant journal bearing using a couple stress fluid as the lubricant. The results obtained are as follows: both the maximum pressure and the load-carrying capacity increase with the increase of the couple stress parameter; the attitude angle and the friction factor decrease when the couple stress parameter increases; and the side leakage flow remains almost constant as the couple stress parameter increases, except for coatings characterized by a low elasticity modulus.

More recently, Lahmar *(8)* analyzed the combined effects of flow rheology (couple stress effect) and fluid-solid interaction (elastic deformation effect) on the static and dynamic performance characteristics of a double-layered journal bearing. It is noticed that all the previous studies have been carried out in isothermal lubrication conditions. Wang, et al. *(9)* investigated the thermohydrodynamic (THD) performance of a finite journal bearing lubricated by oils blended with polymer additives. The authors showed that the lubricants with couple stresses, compared to Newtonian lubricants, produce a lower bearing temperature field.

In the literature, very few studies have been devoted to internal combustion engine connecting rod bearings lubricated with couple stresses fluids. Wang, et al. *(10)* have recently published a work

on the performance of dynamically loaded journal bearings lubricated with couple stress fluids in the case of a gasoline engine. It should be noted that the authors did not provide any information concerning the evolution of power loss, peak pressure, or minimum film thickness during an engine cycle, all of which are key parameters for the design of engine bearings. We present in this paper a complete theoretical study of the behavior of a big end connecting rod bearing dynamic for both the diesel and the gasoline engines, using mineral oils blended with a VI improver as lubricant. The mobility method (Booker *(11)*) has been adapted to the numerical treatment of nonlinear motion equations of the rigid crank pin. The effects of different values of the couple stress parameter on the minimum film thickness, the peak pressure, the flow rate, the power loss, as well as the crank pin trajectories, are investigated.

THEORETICAL ANALYSIS

The Modified Reynolds Equation

On the basis of the V. K. Stokes' micro-continuum theory (Lin *(4)*), when body forces b_i and body couples ℓ_i^* are considered, the motion of the couple stress fluid is governed by the following equations:

$$\frac{D\rho}{Dt} + \rho \frac{\partial u_i}{\partial x_i} = 0 \quad [1]$$

$$\rho \frac{Du_i}{Dt} = \frac{\partial \sigma_{ji}}{\partial x_j} + \rho\, b_i \quad [2]$$

$$M_{ji,j} + e_{ijk}\sigma_{jk} + \rho\, \ell_i^* = 0 \quad [3]$$

where $\frac{D}{Dt}() = \frac{\partial}{\partial t}() + u_j \frac{\partial}{\partial x_j}()$ and $\sigma_{ji} \neq \sigma_{ij}$.

The constitutive equations for the couple-stress fluids are given as (Lin *(4)*):

$$\sigma_{ij} = \left(-p + \lambda \frac{\partial u_k}{\partial x_k}\right)\delta_{ij} + \mu\left(\frac{\partial u_i}{\partial x_j} + \frac{\partial u_j}{\partial x_i}\right) - \frac{1}{2} e_{ijk} M_{rk,r} \quad [4]$$

$$M_{rk} = \frac{1}{3} M_{nn}\delta_{rk} + 4\eta\omega_{k,r}^* + 4\eta'\omega_{r,k}^* \quad [5]$$

where $\lambda = -\frac{2\mu}{3}$ (G. Stokes' hypothesis) and $\omega_i^* = \frac{1}{2} e_{irs}\frac{\partial u_s}{\partial x_r}$ is the ith component of the vorticity vector.

The problem to be considered is a finite connecting rod journal bearing, as shown in Fig. 1, lubricated with an incompressible couple-stress fluid; i.e.,

$$\frac{\partial u}{\partial x} + \frac{\partial v}{\partial y} + \frac{\partial w}{\partial z} = 0 \quad [6]$$

If we now consider the case where λ, μ, η, and η' are constants, the conservation of momentum neglecting the body forces and body couples is given by Stokes *(1)*:

$$\rho\left(\frac{\partial u}{\partial t} + u\frac{\partial u}{\partial x} + v\frac{\partial u}{\partial y} + w\frac{\partial u}{\partial z}\right) = -\frac{\partial p}{\partial x} + \mu\left(\frac{\partial^2 u}{\partial x^2} + \frac{\partial^2 u}{\partial y^2} + \frac{\partial^2 u}{\partial z^2}\right) - \eta\left(\frac{\partial^4 u}{\partial x^4} + \frac{\partial^4 u}{\partial y^4} + \frac{\partial^4 u}{\partial z^4}\right) - 2\eta\left(\frac{\partial^4 u}{\partial x^2\partial y^2} + \frac{\partial^4 u}{\partial x^2\partial z^2} + \frac{\partial^4 u}{\partial y^2\partial z^2}\right) \quad [7a]$$

$$\rho\left(\frac{\partial v}{\partial t} + u\frac{\partial v}{\partial x} + v\frac{\partial v}{\partial y} + w\frac{\partial v}{\partial z}\right) = -\frac{\partial p}{\partial y} + \mu\left(\frac{\partial^2 v}{\partial x^2} + \frac{\partial^2 v}{\partial y^2} + \frac{\partial^2 v}{\partial z^2}\right) - \eta\left(\frac{\partial^4 v}{\partial x^4} + \frac{\partial^4 v}{\partial y^4} + \frac{\partial^4 v}{\partial z^4}\right) - 2\eta\left(\frac{\partial^4 v}{\partial x^2\partial y^2} + \frac{\partial^4 v}{\partial x^2\partial z^2} + \frac{\partial^4 v}{\partial y^2\partial z^2}\right) \quad [7b]$$

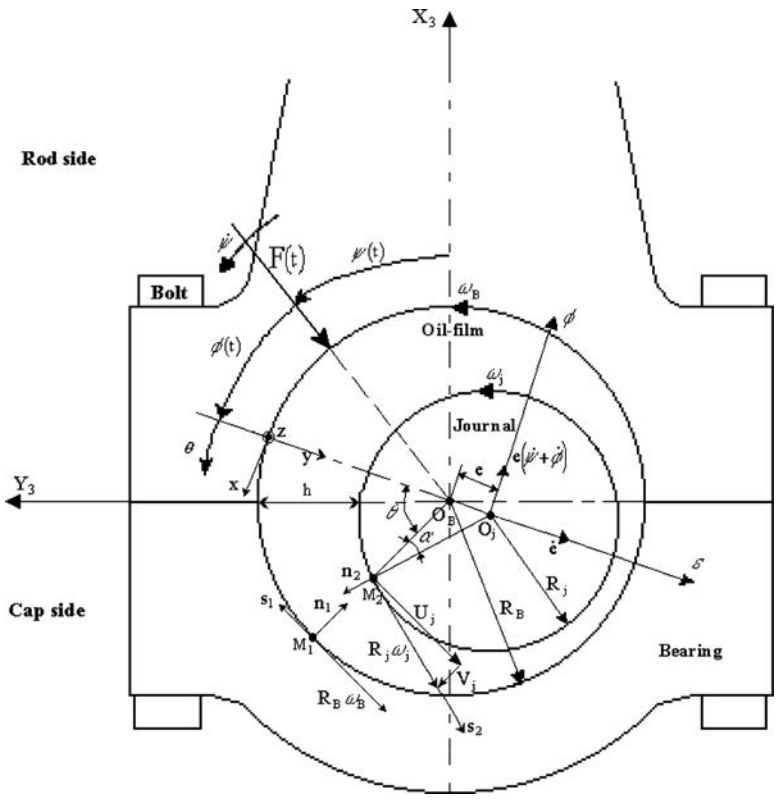

Fig. 1—Connecting rod big end journal bearing and coordinate system.

$$\rho\left(\frac{\partial w}{\partial t}+u\frac{\partial w}{\partial x}+v\frac{\partial w}{\partial y}+w\frac{\partial w}{\partial z}\right)$$
$$=-\frac{\partial p}{\partial z}+\mu\left(\frac{\partial^2 w}{\partial x^2}+\frac{\partial^2 w}{\partial y^2}+\frac{\partial^2 w}{\partial z^2}\right)-\eta\left(\frac{\partial^4 w}{\partial x^4}+\frac{\partial^4 w}{\partial y^4}+\frac{\partial^4 w}{\partial z^4}\right)$$
$$-2\eta\left(\frac{\partial^4 w}{\partial x^2\partial y^2}+\frac{\partial^4 w}{\partial x^2\partial z^2}+\frac{\partial^4 w}{\partial y^2\partial z^2}\right) \quad [7c]$$

where ρ is the fluid density, u, v, and w are the velocity components, t is the time, p is the pressure, μ is the classical shear viscosity, and η is a new material parameter responsible for the couple stress property.

Note that the dimensions of the material constants λ and μ are those of viscosity ($ML^{-1}T^{-1}$), whereas the dimensions of η and η' are those of momentum (MLT^{-1}). The λ and μ given here should not be taken to be the same constants as in the non-polar case. The ratio η/μ has the dimension of the length squared. In the following, we denote this material constant by ℓ, where $\ell = (\eta/\mu)^{1/2}$. Some experiments for determining the material constants μ, η, and η' for incompressible fluids are given in Stokes *(1)*. Physically, the quantity ℓ can be regarded as a characteristic length of the additives that are added to the base oil and can be polymers or co-polymers.

Making the usual assumption of hydrodynamic lubrication applicable to thin films, the momentum equations [7] are reduced to (see Appendix A for details):

$$\begin{cases}\dfrac{\partial^4 u}{\partial y^4}-\dfrac{1}{\ell^2}\dfrac{\partial^2 u}{\partial y^2}=-\dfrac{1}{\eta}\dfrac{\partial p}{\partial x}\\ 0=\dfrac{\partial p}{\partial y}\\ \dfrac{\partial^4 w}{\partial y^4}-\dfrac{1}{\ell^2}\dfrac{\partial^2 w}{\partial y^2}=-\dfrac{1}{\eta}\dfrac{\partial p}{\partial z}\end{cases} \quad [8]$$

where $\ell = (\eta/\mu)^{1/2}$

The general solutions to equations [8] are

$$\begin{cases}u = A_0 + A_1 y + B_1 Cosh\left(\dfrac{y}{\ell}\right) + B_2 Sinh\left(\dfrac{y}{\ell}\right) + \dfrac{1}{2\mu}\dfrac{\partial p}{\partial x}y^2\\ w = C_0 + C_1 y + D_1 Cosh\left(\dfrac{y}{\ell}\right) + D_2 Sinh\left(\dfrac{y}{\ell}\right) + \dfrac{1}{2\mu}\dfrac{\partial p}{\partial z}y^2\end{cases} \quad [9a]$$

The boundary conditions at the bearing surfaces ($y = 0$) and the journal surface ($y = h$) are:

$$u(x,0,z) = U_b \quad [10a]$$
$$w(x,0,z) = 0 \quad [10b]$$
$$\left.\frac{\partial^2 u}{\partial y^2}\right|_{y=0} = 0 \quad [10c]$$
$$\left.\frac{\partial^2 w}{\partial y^2}\right|_{y=0} = 0 \quad [10d]$$
$$u(x,h,z) = U_j \quad [10e]$$
$$w(x,h,z) = 0 \quad [10f]$$
$$\left.\frac{\partial^2 u}{\partial y^2}\right|_{y=h} = 0 \quad [10g]$$
$$\left.\frac{\partial^2 w}{\partial y^2}\right|_{y=h} = 0 \quad [10h]$$

Conditions [10a] and [10e] are the no-slip velocity conditions, and conditions [10c], [10d], [10g], and [10h] result from the fact that the couple stresses ($-2\eta\frac{\partial^2 u}{\partial y^2}$) and ($-2\eta\frac{\partial^2 w}{\partial y^2}$) vanish at the solid boundary. Using the above boundary conditions, the fluid velocity components u and w and their derivatives are

$$u = U_b + (U_j - U_b)\frac{y}{h} + \frac{1}{2\mu}\frac{\partial p}{\partial x} \times\left\{y(y-h)+2\ell^2\left[1-\frac{\cosh\left(\frac{2y-h}{2\ell}\right)}{\cosh\left(\frac{h}{2\ell}\right)}\right]\right\} \quad [11a]$$

$$w = \frac{1}{2\mu}\frac{\partial p}{\partial z}\left\{y(y-h)+2\ell^2\left[1-\frac{\cosh\left(\frac{2y-h}{2\ell}\right)}{\cosh\left(\frac{h}{2\ell}\right)}\right]\right\} \quad [11b]$$

$$\begin{cases}\dfrac{\partial u}{\partial y}=\dfrac{U_{j-}U_b}{h}+\dfrac{1}{2\mu}\dfrac{\partial p}{\partial x}\left[2y-h-2\ell\dfrac{\sinh\left(\frac{2y-h}{2\ell}\right)}{\cosh\left(\frac{h}{2\ell}\right)}\right]\\ \dfrac{\partial^2 u}{\partial y^2}=\dfrac{1}{2\mu}\dfrac{\partial p}{\partial x}\left[2-2\dfrac{\cosh\left(\frac{2y-h}{2\ell}\right)}{\cosh\left(\frac{h}{2\ell}\right)}\right]\\ \dfrac{\partial^3 u}{\partial y^3}=-\dfrac{1}{\mu}\dfrac{\partial p}{\partial x}\dfrac{1}{\ell}\dfrac{\sinh\left(\frac{2y-h}{2\ell}\right)}{\cosh\left(\frac{h}{2\ell}\right)}\end{cases} \quad [12a]$$

$$\begin{cases}\dfrac{\partial w}{\partial y}=\dfrac{1}{2\mu}\dfrac{\partial p}{\partial z}\left[2y-h-2\ell\dfrac{\sinh\left(\frac{2y-h}{2\ell}\right)}{\cosh\left(\frac{h}{2\ell}\right)}\right]\\ \dfrac{\partial^2 w}{\partial y^2}=\dfrac{1}{2\mu}\dfrac{\partial p}{\partial z}\left[2-2\dfrac{\cosh\left(\frac{2y-h}{2\ell}\right)}{\cosh\left(\frac{h}{2\ell}\right)}\right]\\ \dfrac{\partial^3 w}{\partial y^3}=-\dfrac{1}{\mu}\dfrac{\partial p}{\partial z}\dfrac{1}{\ell}\dfrac{\sinh\left(\frac{2y-h}{2\ell}\right)}{\cosh\left(\frac{h}{2\ell}\right)}\end{cases} \quad [12b]$$

Substituting the expressions of the velocity components u and w, and integrating the continuity equation [6] with respect to y using the boundary conditions for v given by:

$$\begin{aligned}v(x,0,z) &= 0\\ v(x,h,z) &= V_j\end{aligned} \quad [13]$$

the modified Reynolds equation is

$$\frac{\partial}{\partial x}\left(G(\ell,h)\frac{\partial p}{\partial x}\right)+\frac{\partial}{\partial z}\left(G(\ell,h)\frac{\partial p}{\partial z}\right) = 6\mu\left[(U_b-U_j)\frac{\partial h}{\partial x}+h\frac{\partial}{\partial x}(U_b+U_j)+2V_j\right] \quad [14]$$

where:

$$G(\ell,h) = h^3 - 12\ell^2\left[h-2\ell\tanh\left(\frac{h}{2\ell}\right)\right] \quad [15]$$

and

$$U_j = \dot{e}\sin\theta - e(\dot{\phi}+\dot{\psi})\cos\theta + \omega_j R_j - \dot{e}\cos\theta\frac{\partial h}{\partial x} - e(\dot{\phi}+\dot{\psi})\sin\theta\frac{\partial h}{\partial x} \quad [16]$$

$$V_j = \dot{e}\cos\theta + e(\dot{\phi}+\dot{\psi})\sin\theta + \omega_j R_j \frac{\partial h}{\partial x} + \dot{e}\sin\theta\frac{\partial h}{\partial x} - e(\dot{\phi}+\dot{\psi})\cos\theta\frac{\partial h}{\partial x} \quad [17]$$

$$U_b = \omega_b R_b \quad [18]$$

The pressure field must satisfy the modified Reynolds equation and the following boundary conditions:

$$p|_{z=\pm L/2} = 0,\ p|_{\theta=0} = p|_{\theta=2\pi} \quad [19a]$$

$$p|_{\theta=\theta_2} = \frac{\partial p}{\partial\theta}\Big|_{\theta=\theta_2} = 0 \quad [19b]$$

where θ_2 represents the location of the starting of the cavitation region.

Equations [19b], the so-called Reynolds boundary conditions, are often used in numerical simulations of hydrodynamic lubrication problems. They are nevertheless unable to exactly predict the location of film reformation. These conditions lead to fairly good agreement with experimental data, particularly at large operating eccentricity. Indeed, Vincent, et al. *(12)* demonstrated through a theoretical investigation that the characteristics (the crank pin trajectories, the minimum film thickness, the pressure profile, the friction torque, and the axial flow rate) of the Ruston and Hornsby diesel engine connecting rod bearing calculated using the Reynolds boundary conditions and the Elrod-Adams (mass conserving) cavitation are quite similar over the entire engine cycle.

Mobility Method

In this section, we briefly review the mobility method. This method is an efficient tool to obtain a quick solution of dynamically loaded cylindrical journal bearing problems. The fluid film pressure distributions can be calculated from the solution of the modified Reynolds equation if the operating eccentricity is specified. Then, the fluid film supported load can be obtained from the integration of the pressure distributions over the bearing surface. This is a so-called direct problem. However, for journal bearings belonging to reciprocating machinery, such as internal combustion engines and compressors, usually the inverse problem needs to be solved; i.e., dynamical loads applied on the bearing are known but the eccentricities of the journal need to be calculated. The inverse problem is more difficult to solve than the direct problem, because it has to be solved through an iterative procedure, which makes the analysis more complex and time-consuming.

There have been various attempts to quickly predict the journal center trajectory during the load cycle. In 1965, Booker *(11)* suggested the so-called mobility method, which is an efficient tool to obtain a quick solution of dynamically loaded cylindrical journal bearing problems.

Introducing the following dimensionless variables:

$$\theta = \frac{x}{R},\quad \tilde{h} = \frac{h}{C},\quad \tilde{z} = \frac{z}{L}, \tilde{\ell} = \frac{\ell}{C},\quad \varepsilon = \frac{e}{C},\quad \tilde{p} = p\frac{LD}{F} \quad [20]$$

where ε is the eccentricity ratio equation [14] becomes:

$$\frac{\partial}{\partial\theta}\left\{[\tilde{h}^3 - \tilde{f}(\tilde{h},\tilde{\ell})]\frac{\partial\tilde{p}}{\partial\theta}\right\} + \left(\frac{R}{L}\right)^2\frac{\partial}{\partial\tilde{z}}\left\{[\tilde{h}^3 - \tilde{f}(\tilde{h},\tilde{\ell})]\frac{\partial\tilde{p}}{\partial\tilde{z}}\right\} = \frac{12\mu LD}{F\left(\frac{C}{R}\right)^2}[(\dot{\phi}-\bar{\omega})\varepsilon\sin\theta + \dot{\varepsilon}\cos\theta] \quad [21]$$

where:

$$\tilde{f}(\tilde{h},\tilde{\ell}) = 12\tilde{\ell}^2\left[\tilde{h} - 2\tilde{\ell}\tanh\left(\frac{\tilde{h}}{2\tilde{\ell}}\right)\right] \quad [22]$$

and $\bar{\omega}$ is the average angular velocity of journal and sleeve (bearing) relative to the load line defined as: $\bar{\omega} = \frac{\omega_j+\omega_b}{2} - \dot{\psi}$. Note that $\bar{\omega}$ is obtained from a kinematic analysis of the crank-slider mechanism (Booker *(11)*). As $\tilde{\ell} \to 0$, the function $\tilde{f}(\tilde{h},\tilde{\ell})$ defined in Eq. [22] approaches zero and the modified Reynolds equation [21] reduces to the classical form of the Newtonian lubricant case.

According to the mobility technique, the components of the velocity vector $\dot{\varepsilon}$ and $\varepsilon(\dot{\phi}-\bar{\omega})$ appearing on the RHS of the modified Reynolds equation [21] can be expressed as:

$$\dot{\varepsilon} = \frac{F(C/R)^2}{\mu LD}M_\varepsilon\left(\varepsilon, \frac{L}{D}, \phi, \theta_1, \theta_2\right) \quad [23a]$$

$$\varepsilon(\dot{\phi}-\bar{\omega}) = \frac{F(C/R)^2}{\mu LD}M_\phi\left(\varepsilon, \frac{L}{D}, \phi, \theta_1, \theta_2\right) \quad [23b]$$

where M_ε and M_ϕ are the components of the mobility vector M defined by Booker *(11)*:

$$\begin{Bmatrix} M_\varepsilon \\ M_\phi \end{Bmatrix} = M\begin{Bmatrix} \cos\alpha_M \\ -\sin\alpha_M \end{Bmatrix} \quad [24]$$

α_M being the angle between the mobility vector and the eccentricity direction.

Introducing the non-dimensional pressure $\tilde{p} = \tilde{p}^* M$, Eq. [21] becomes

$$\frac{\partial}{\partial\theta}\left\{[\tilde{h}^3 - \tilde{f}(\tilde{h},\tilde{\ell})]\frac{\partial\tilde{p}^*}{\partial\theta}\right\} + \left(\frac{R}{L}\right)^2\frac{\partial}{\partial\tilde{z}}\left\{[\tilde{h}^3 - \tilde{f}(\tilde{h},\tilde{\ell})]\frac{\partial\tilde{p}^*}{\partial\tilde{z}}\right\} = 12\cos(\theta+\alpha_M) \quad [25]$$

The mobility method enables a full orbit of the journal bearing center to be calculated very rapidly, without reiterative calculations at each time step. However, the method has a number of limitations, which make it inappropriate in the analysis of the following cases:

- the bearing is not fully flooded by the lubricant (starvation effects);
- the density and viscosity of lubricant are pressure dependent (compressibility and piezo-viscosity effects);
- the bearing is partially grooved in a circumferential direction.

Furthermore, only cylindrical journal bearings may be conveniently treated by this technique.

Mean Flow Velocities and Side Leakage Flow

The mean flow velocities $\bar{u}$ and $\bar{w}$ are determined by the following relationships:

$$\bar{u} = \frac{1}{h}\int_0^h u\,dy = \frac{U_j+U_b}{2} - \frac{1}{12\mu}\frac{\partial p}{\partial x} \times\left[h^2 - 12\ell^2 + \frac{24\ell^3 Tanh\left(\frac{h}{2\ell}\right)}{h}\right] \quad [26a]$$

$$\bar{w} = \frac{1}{h}\int_0^h w\,dy = -\frac{1}{12\mu}\frac{\partial p}{\partial x} \times\left[h^2 - 12\ell^2 + \frac{24\ell^3 Tanh\left(\frac{h}{2\ell}\right)}{h}\right] \quad [26b]$$

TABLE 1—RUSTON AND HORNSBY 6 VEB-X MK III DIESEL ENGINE PARAMETERS AND GROOVED CONNECTING-ROD BEARING DATA *(11)*

Parameter	Symbol	Unit	Value
Engine speed	ω_2	rad/s	$-20 \times \pi$
Crankshaft-arm length	ℓ_2	m	0.184
Connecting-rod length	ℓ_3	m	0.782
Bearing diameter	D	m	0.2032
Bearing length	L	m	0.127
Radial clearance	C	m	82.55×10^{-6}
Base-oil dynamic viscosity	μ	Pa.s	0.015
Engine cycle (crank angle)		degrees	720
Ambient pressure		Pa	0.0
Circumferential groove width		m	0.0127

The side leakage flow is found from

$$Q_z = \left| \int_{\theta_1}^{\theta_2} [h\bar{w}]_{z=L/2} \, Rd\theta \right| + \left| \int_{\theta_1}^{\theta_2} [h\bar{w}]_{z=-L/2} \, Rd\theta \right| \qquad [27]$$

Power Loss

The power loss, which represents the energy dissipation due to the viscous shear stress, can be obtained from

$$P = \int_{\frac{L}{2}}^{\frac{L}{2}} \int_0^h \int_{\theta 1}^{\theta_2} \Phi Rd\theta dy dz \qquad [28]$$

where Φ is the specific viscous dissipation function defined as:

$$\Phi = \mu \left\{ \left[\left(\frac{\partial u}{\partial y} \right)^2 + \left(\frac{\partial w}{\partial y} \right)^2 \right] - \ell^2 \left(\frac{\partial u}{\partial y} \frac{\partial^3 u}{\partial y^3} + \frac{\partial w}{\partial y} \frac{\partial^3 w}{\partial y^3} \right) \right\}$$

$$= \mu \left[\left(\frac{\partial u}{\partial y} \right)^2 + \left(\frac{\partial w}{\partial y} \right)^2 \right] - \eta \left(\frac{\partial u}{\partial y} \frac{\partial^3 u}{\partial y^3} + \frac{\partial w}{\partial y} \frac{\partial^3 w}{\partial y^3} \right) \qquad [29]$$

As ℓ tends to zero (Newtonian case), Eq. [29] reduces to,

$$\Phi = \mu \left[\left(\frac{\partial u}{\partial y} \right)^2 + \left(\frac{\partial w}{\partial y} \right)^2 \right] \qquad [30]$$

The total power loss is the sum of two contributions, the Hagen-Poiseuille term, arising from pressure gradients, and the Couette term, due to the journal and bearing rotations:

$$\mathrm{P}_{Hagen-Poiseuille} = \int_{-\frac{L}{2}}^{\frac{L}{2}} \int_{\theta_1}^{\theta_2} \frac{G(h,\ell)}{12\mu} \left[\left(\frac{\partial p}{R\partial\theta} \right)^2 + \left(\frac{\partial p}{\partial z} \right)^2 \right] Rd\theta dz \qquad [31]$$

$$\mathrm{P}_{Couette} = \int_{-\frac{L}{2}}^{\frac{L}{2}} \int_{\theta_1}^{\theta_2} \frac{\mu (U_j - U_b)^2}{h} Rd\theta dz \qquad [32]$$

EQUATIONS OF MOTION

Using the (x,y,z) coordinate system, differential equations [23] take the following form:

$$\begin{Bmatrix} \dot{\varepsilon}_x \\ \dot{\varepsilon}_y \end{Bmatrix} = \frac{F\left(\frac{C}{R}\right)^2}{\mu LD} \begin{Bmatrix} M_x \\ M_y \end{Bmatrix} + \bar{\omega} \begin{bmatrix} 0 & -1 \\ 1 & 0 \end{bmatrix} \begin{Bmatrix} \varepsilon_x \\ \varepsilon_y \end{Bmatrix} \qquad [33]$$

where:

$$\begin{Bmatrix} M_x \\ M_y \end{Bmatrix} = \begin{bmatrix} \cos\psi & -\sin\psi \\ \sin\psi & \cos\psi \end{bmatrix} . \begin{bmatrix} \cos\phi_0 & -\sin\phi_0 \\ \sin\phi_0 & \cos\phi_0 \end{bmatrix} \begin{Bmatrix} M_\varepsilon \\ M_\phi \end{Bmatrix} \qquad [34]$$

and

$$\begin{bmatrix} \cos\psi \\ \sin\psi \end{bmatrix} = \frac{1}{|F|} \begin{bmatrix} F_x \\ F_y \end{bmatrix}, \quad \phi_0 = Tan^{-1}\left(\frac{\varepsilon_\eta}{\varepsilon_\xi} \right) \qquad [35]$$

where ϕ_0 is the imposed attitude angle.

The components ε_η and ε_ξ of journal eccentricity ratio are expressed by relations of the form:

$$\begin{Bmatrix} \varepsilon_\xi \\ \varepsilon_\eta \end{Bmatrix} = \begin{bmatrix} \cos\psi & \sin\psi \\ -\sin\psi & \cos\psi \end{bmatrix} \begin{Bmatrix} \varepsilon_x \\ \varepsilon_y \end{Bmatrix} \qquad [36]$$

COMPUTATION PROCEDURE

The solution of the hydrodynamic lubrication problem in the dynamically loaded bearings is obtained by the following iterative procedure:

1. Select the input parameters of the problem: L, D, C, μ, η, ω_2, ℓ_2, ℓ_3; applied load components F_x, F_y; time step Δt or increment of crankshaft rotation $\Delta\theta_C$; initial crank angle θ_{C_0} or initial time t_0; mesh characteristics N_θ and N_z; over-relaxation factor Ω; convergence criteria; and the maximum number of iterations for the pressure solution.
2. Choose initial values of ε_x, ε_y, $t = t_0$.
3. Compute imposed attitude angle ϕ_0 (Eqs [35] and [36]).
4. Choose initial value of α_M.

TABLE 2—COMPARISON BETWEEN EXPERIMENTAL AND THEORETICAL MINIMUM OIL-FILM THICKNESS FOR RUSTON & HORNSBY 6 VEB-X MK III CONNECTING ROD BEARING WITH FULL CIRCUMFERENTIAL GROOVE (MARTIN *(15)*)

Source	Type	h_{min} ($\times 10^{-6}$ m)	Crank angle after TDC (degrees)
Glacier Metal Co.	Experimental		
- From R & H 6 VEB engine		2.8	240
- From dynamic similarity machine		3.3	270
General Electric Co, UK	Computed		
- Ritchie (Finite bearing)		3.6	275
- Ritchie (Optimized short bearing)		3.3	272
General Motors Research	Computed		
- Finite element program		3.48	—
- Goenka (rapid curve-fit program)		3.48	—
Glacier Metal Co.	Computed		
- Jones (finite bearing)		3.57	—
- Jones (with film history)		2.29	—
Present study	Computed		
(2-D mobility method)		3.574	275.5

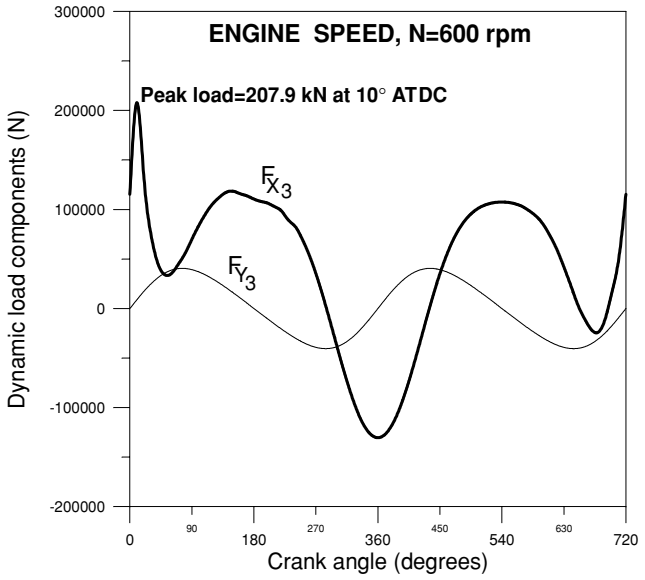

Fig. 2—Loading on the Ruston and Hornsby diesel engine connecting rod big end bearing relative to connecting rod axis.

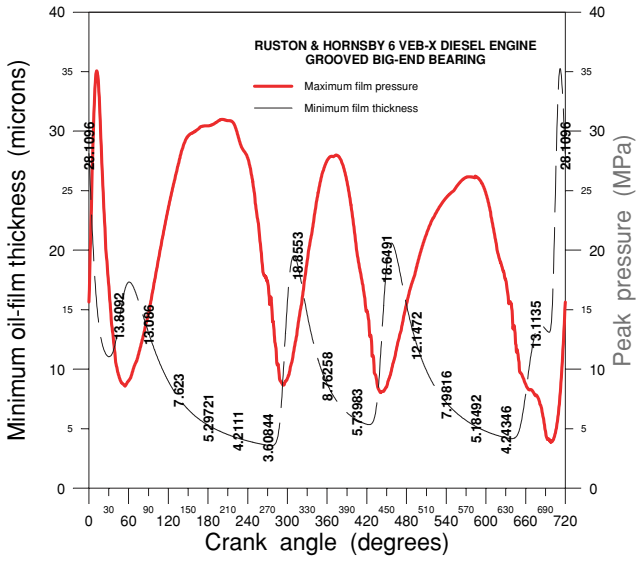

Fig. 4—Minimum film thickness and maximum film pressure as functions of crank angle.

5. Solve the modified Reynolds equation (Eq. [25]) for the pressure field $\tilde{p}^*$ using the finite difference method with successive over-relaxation scheme.
6. Calculate the dimensionless load components

$$\begin{Bmatrix} \tilde{W}_\varepsilon \\ \tilde{W}_\phi \end{Bmatrix} = \int_{1/2}^{1/2} \int_{\theta_1}^{\theta_2} \tilde{p}^* \begin{Bmatrix} \cos\theta \\ \sin\theta \end{Bmatrix} d\theta d\tilde{z}$$

and attitude angle $\phi = Tan^{-1}(-\tilde{W}_\phi/\tilde{W}_\varepsilon)$. The above integrals were evaluated by means of the trapezoidal formula.

7. Check the convergence criterion $|\phi - \phi_0| \leq 10^{-3}$ If convergence is not achieved, then calculate a new value of α_M by a linear interpolation method and return to step 5.
8. Calculate the mobility factor $M = \frac{2}{(\bar{W}_\varepsilon^2 + \bar{W}_\phi^2)^{1/2}}$, M_ε and M_ϕ using Eq. [24].
9. Calculate the velocity components of the journal center $\dot{\varepsilon}_x$ and$\dot{\varepsilon}_y$ using Eqs. [33] and [34].
10. Calculate the displacement components of the journal center by means of the Euler scheme: $\varepsilon_x = \varepsilon_x + \Delta t \dot{\varepsilon}_x$ and $\varepsilon_y = \varepsilon_y + \Delta t \dot{\varepsilon}_y$ where $\Delta t = \Delta\theta_C/\omega_2$.

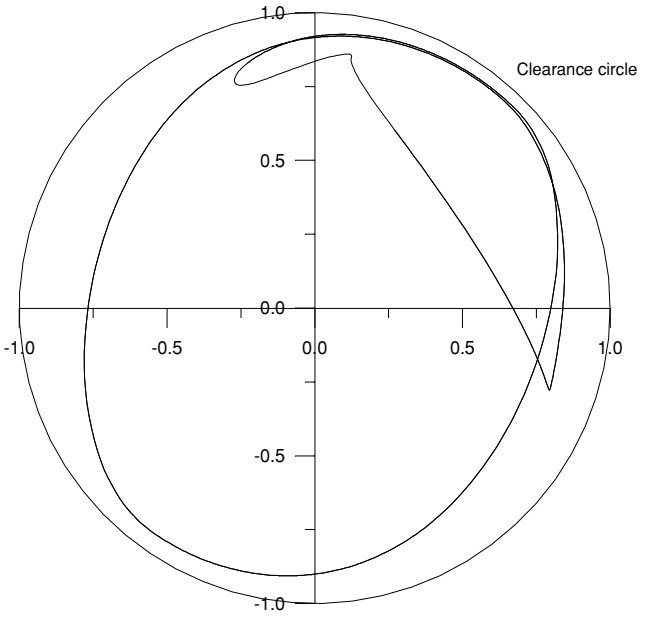

Fig. 3—Predicted journal center cyclic path for the grooved Ruston and Hornsby 6 VEB connecting-rod bearing lubricated with Newtonian fluid ($\bar{\ell} = 0.0$).

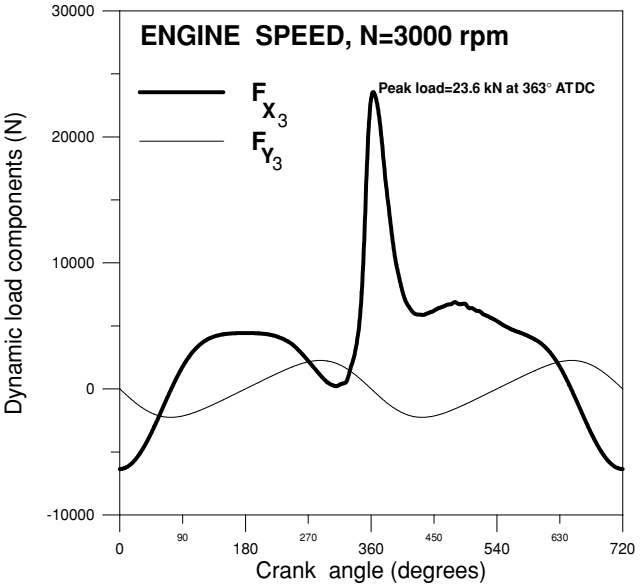

Fig. 5—Loading on the gasoline engine connecting rod big end bearing relative to connecting rod axis.

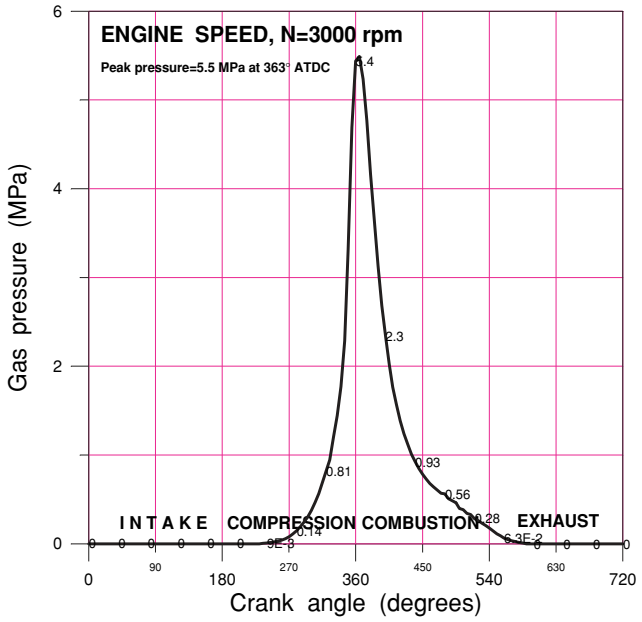

Fig. 6—Gas pressure measured in the combustion chamber versus crank angle for the gasoline engine.

11. Code the nodes for which the hydrodynamic pressure is positive. This step is necessary to evaluate the power loss, etc.
12. Calculate the performance characteristics such as minimum film thickness, peak pressure, axial flow rate, power loss.
13. If $t < t_{\text{lim}}$, then set $t = t + \Delta t$ and use new ε_x and new ε_y in step 3, and repeat the entire process until the cycle repeats itself.

In the calculations, the oil film domain is discretized, the non-dimensional Reynolds' equation [25] is substituted by the linear system of finite difference equations, and solved by the successive over relaxations (S.O.R.) method. The Reynolds film rupture conditions [19b] are satisfied by applying the Christopherson's algorithm *(13)*. To ensure convergence in the iterative procedure, the value of over-relaxation coefficient Ω is fixed to 1.80. Applying the S.O.R method, the finite difference form of the Reynolds' equation will be

$$\tilde{p}_{i,j}^{*(k+1)} = (1-\Omega)\tilde{p}_{i,j}^{*(k)} + \Omega\Big(a_{i,j}\tilde{p}_{i+1,j}^{*(k)} + b_{i,j}\tilde{p}_{i-1,j}^{*(k+1)} + c_{i,j}\tilde{p}_{i,j+1}^{*(k)} + d_{i,j}\tilde{p}_{i,j-1}^{*(k+1)} + e_{i,j}\Big) \quad [37]$$

where (k) and $(k+1)$ express the steps of iterations.

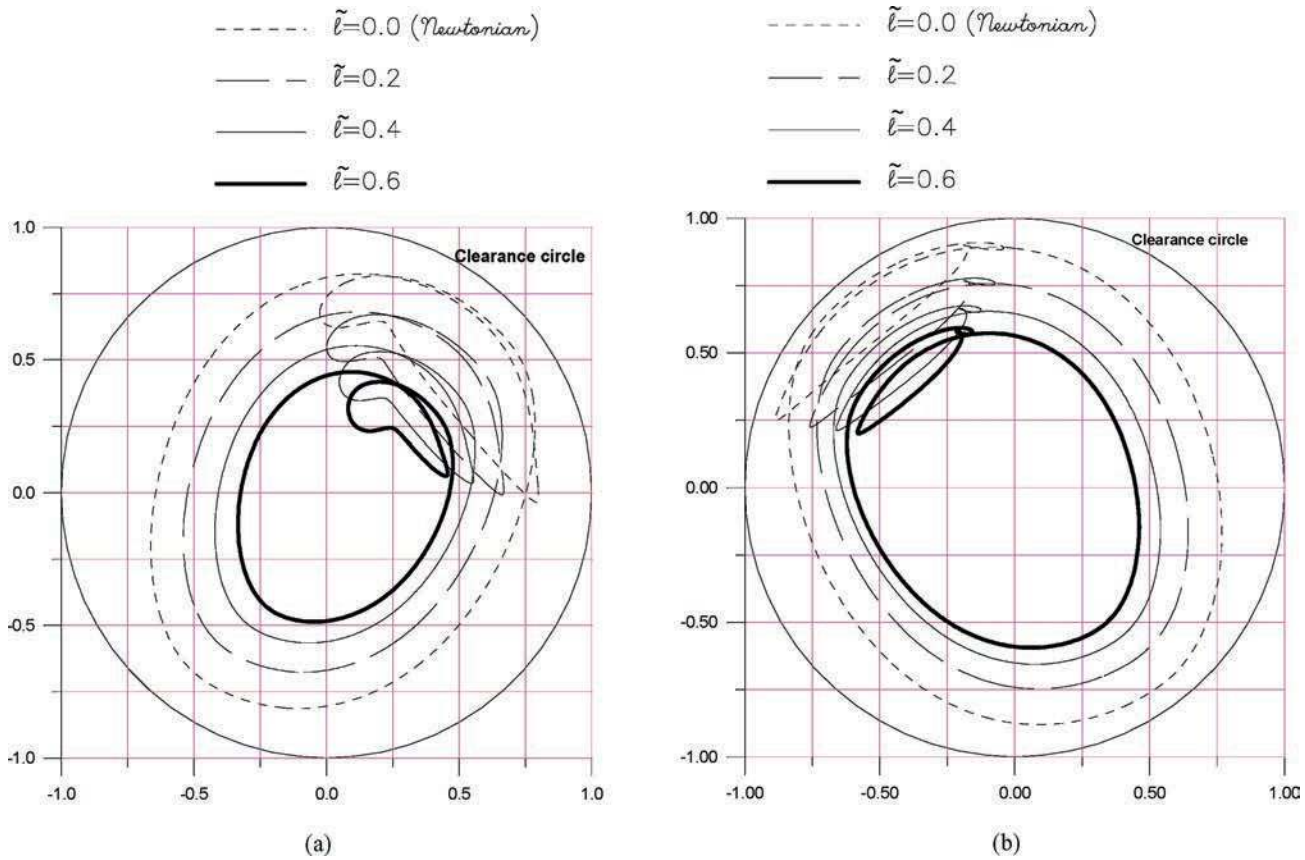

Fig. 7—Journal center orbits over an engine cycle for different values of the couple stresses parameter; (a) diesel engine, (b) gasoline engine.

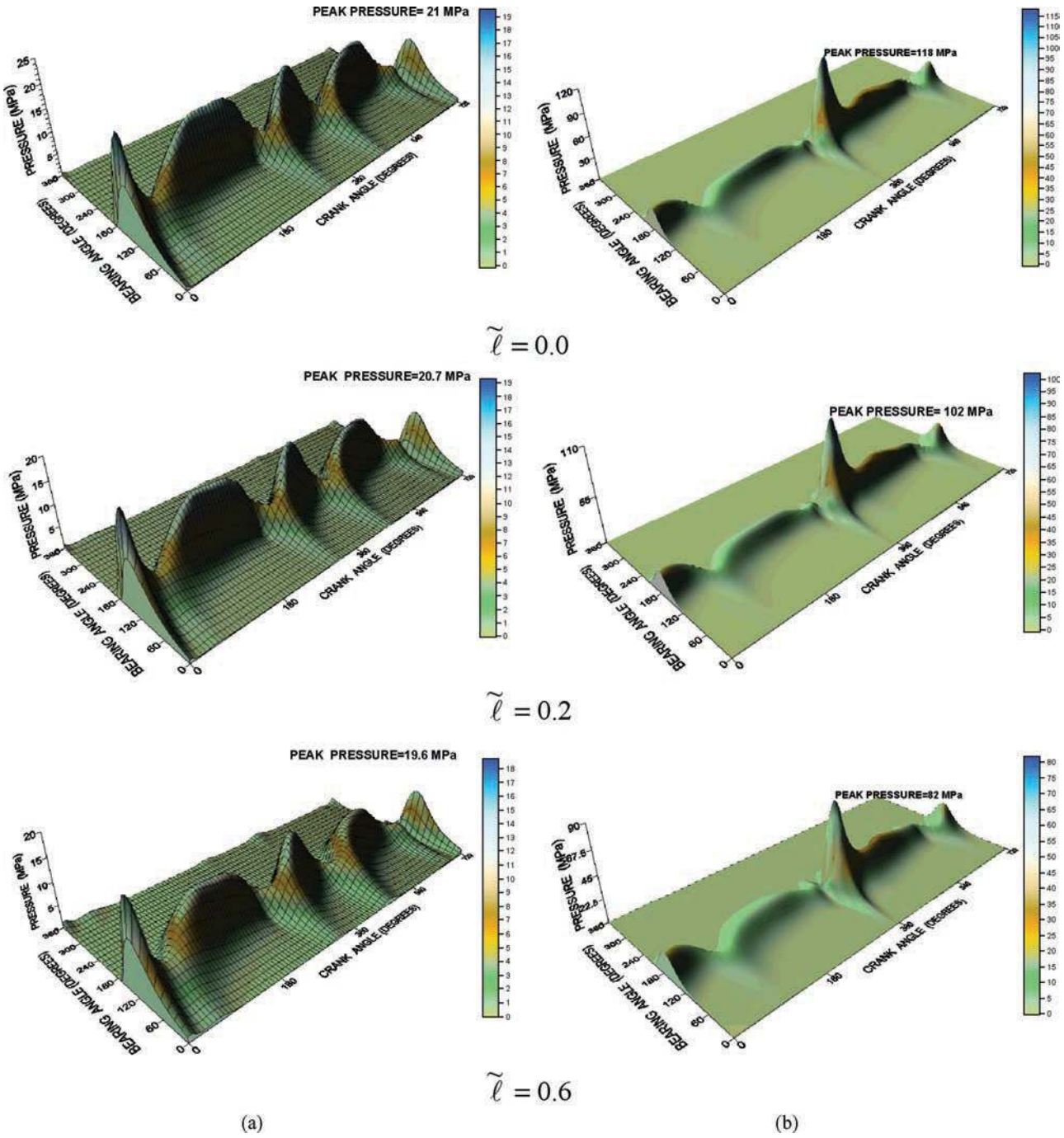

Fig. 8—Oil-film pressure distribution as a function of time for both diesel and gasoline engines; (a) diesel engine, (b) gasoline engine.

The process of iteration will be completed when the error is smaller than a prescribed value, ε_p, which is given by

$$\varepsilon_p = \max \left| \frac{\tilde{p}_{i,j}^{*(k+1)} - \tilde{p}_{i,j}^{*(k)}}{\tilde{p}_{i,j}^{*(k+1)}} \right| \leq 10^{-5} \qquad [38]$$

To accurately predict the crank pin center orbit, the considered mesh had 61×21 nodes in the circumferential and axial directions, respectively, and a time step corresponding to 0.5 degrees of crank rotation was used.

RESULTS AND DISCUSSION

The present analysis has been incorporated into a Fortran program that accepts bearing data and the external forces for main, big end, and small end bearings of diesel and gasoline engines. The computed results include bearing center orbits, variations of the

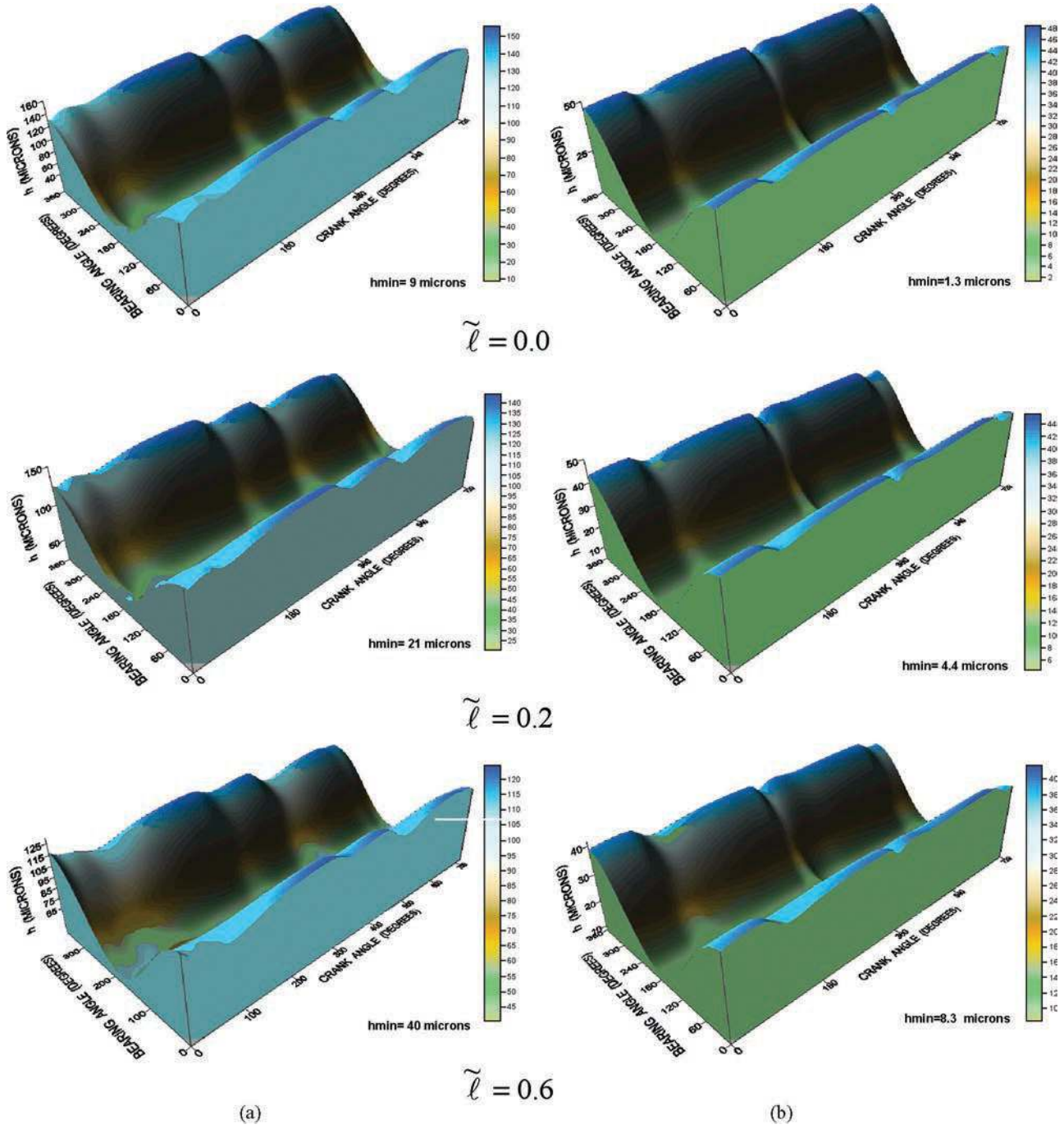

Fig. 9—Film thickness distribution as a function of time for both diesel and gasoline engines; (a) diesel engine, (b) gasoline engine.

minimum film thickness, the peak pressure, the power dissipation, and the axial flow versus the crank angle.

Validation

In order to verify the validity of the computer program, the test data given in Campbell et al. *(14)* for a Ruston and Hornsby 6 VEB-X Mk III big end bearing were used. The bearing characteristics are given in Table 1 and the load on the connecting rod is shown in Fig. 2. This load includes both the gas pressure and the inertia loading whose maximum value is about 207,900 N at 10° crank angle (0° represents the top-dead-center (T.D.C) position and the beginning of the expansion or power stroke of the engine). It is interpolated using cubic splines for each 0.5 degrees of crankshaft rotation to faithfully represent the peak loads. The Ruston and Hornsby diesel engine has become something of a standard for comparing different forms of analysis. The bearing has a 360 degree circumferential oil supply groove of 0.0127 m (0.5 in.), width that was modeled by treating each half of the bearing land as a single bearing and assuming that the magnitude of the supply pressure was negligible. By exploiting symmetry it

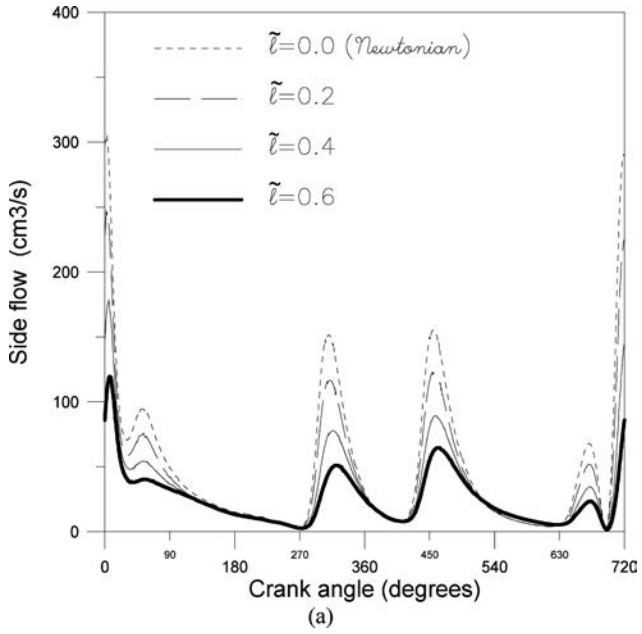

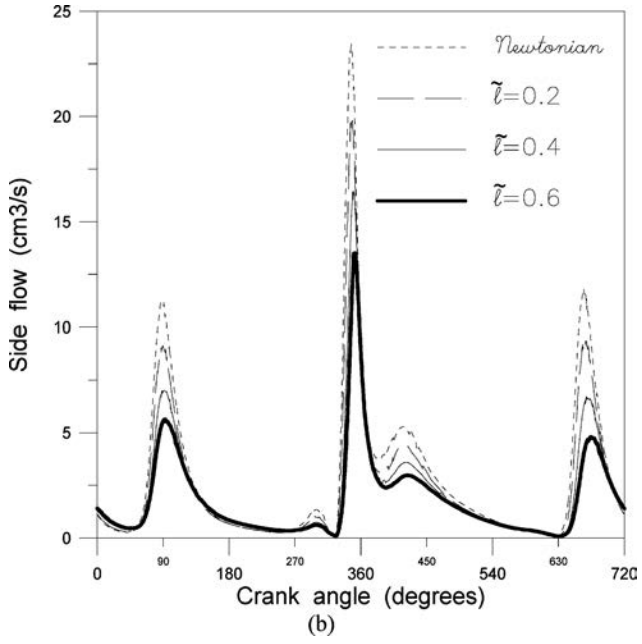

Fig. 10—Side leakage flow over an engine cycle; (a) diesel engine, (b) gasoline engine.

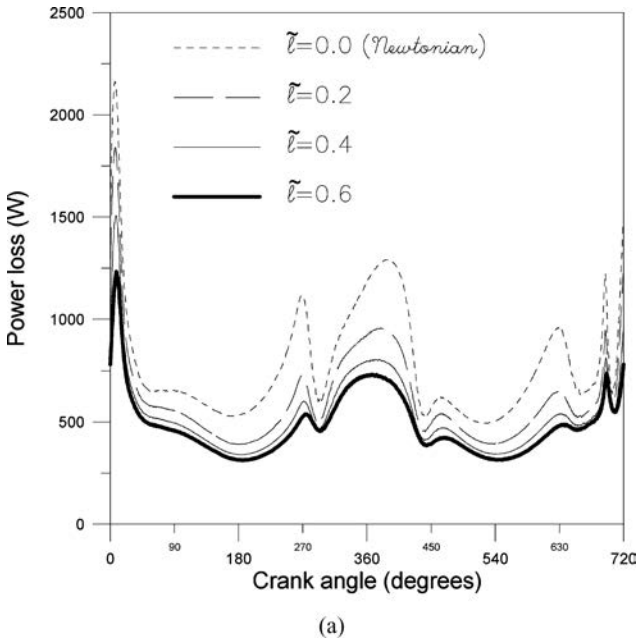

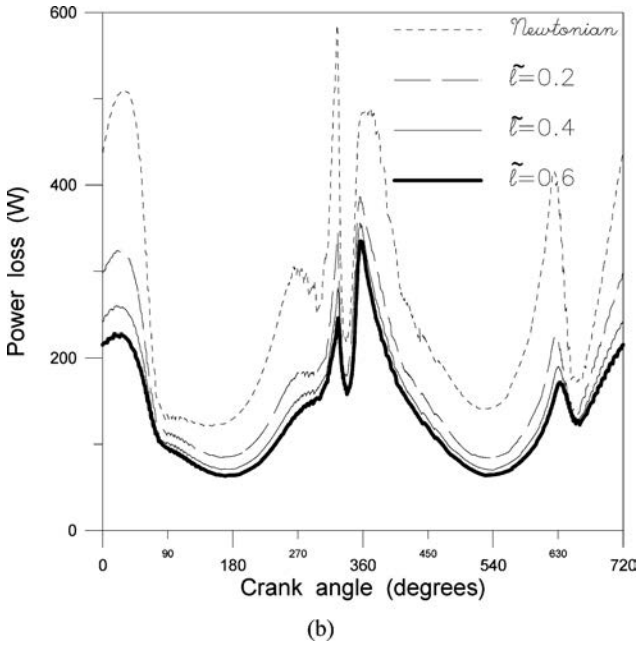

Fig. 11—Power loss over an engine cycle; (a) diesel engine, (b) gasoline engine.

was only necessary to analyze one half of the bearing land. The calculations were performed for the Newtonian case ($\tilde{\ell} = 0.0$).

Figure 3 shows the corresponding steady-state displacement response during the full loading cycle, calculated using the Euler extrapolation with a time step corresponding to 0.5 degrees of crank angle. The general similarity of the locus with those given in Campbell, et al. *(14)* is obvious. The maximum eccentricity ratio of 0.9567 (corresponding to a minimum oil-film thickness of (3.574×10^{-6} m) occurs at 275.5° after T.D.C., and the maximum film pressure of 35.067 MPa occurs at 11.5° after T.D.C. as shown in Fig. 4.

Table 2 gives another check for the correctness of the algorithm and the computer program by comparing the predicted values of the minimum film thickness and the crank angle at which this minimum occurs with those given in table 1 of Martin *(15)*. It may be deduced that the results calculated lie within the scatter of the results obtained by using different techniques (experimental and theoretical).

The computer program was used to study the non-Newtonian effects due to the presence of couple stresses on the dynamic behavior of two ungrooved big end connecting-rod bearings for both diesel and gasoline engines under two different dynamic loadings,

TABLE 3—GASOLINE ENGINE PARAMETERS AND UNGROOVED CONNECTING ROD BEARING DATA

Parameter	Symbol	Unit	Value
Engine speed	ω_2	rad/s	$100\times\pi$
Crankshaft arm length	ℓ_2	m	0.044
Connecting rod length	ℓ_3	m	0.143
Piston diameter	D_p	m	0.083
Piston assembly mass	m_p	kg	0.550
Maximum cylinder pressure		MPa	5.5
Bearing diameter	D	m	0.050
Bearing length	L	m	0.0183
Radial clearance	C	m	25×10^{-6}
Base oil dynamic viscosity	μ	Pa.s	5.9×10^{-3}
Engine cycle (crank angle)		degrees	720
Ambient pressure		Pa	0.0
Connecting rod mass	m_{cr}	kg	0.693
Feed type		—	Oil hole

Figs. 2 and 5. Note that the dynamic loading for the gasoline engine has been obtained from kinematic and dynamic analyses of the crank-slider system using relevant gas pressure in the combustion chamber (Fig. 6) and considering all the elements as rigid. All the data are reported in Tables 1 and 3. In order to visualize the changes due to the presence of the polymer additives, a parametric study has been performed.

Crank Pin Center Orbits

Figure 7 shows the influence of the couple stress parameter on the journal center orbits for both diesel and gasoline engines. We note that increasing this parameter decreases the shaft trajectories in both cases. Adding polymers in a lubricant decreases the oil-film pressure and increases the minimum film thickness (see Figs. 8 and 9). This moves the shaft center orbits towards the bushing center. The orbits calculated for the various values of the couple-stress parameter have the same shapes.

Minimum Oil-Film Thickness and Peak Hydrodynamic Pressure

As the minimum film thickness increases with the increase of the couple stress parameter, we obtain a lower maximum film pressure compared to the Newtonian case as depicted in Figs. 8 and 9.

Side Leakage Flow

The side leakage flow (Fig. 10) is obtained by integration of the mean velocity of the fluid at the bearing edges. As expected, this flow rate decreases with the increase of the couple stress parameter. This difference is more pronounced especially at the firing time.

Power Loss

It is well known that in both gasoline and diesel engines the power loss is an important economic factor. Figure 11 shows clearly the importance of polymer additives in this specific case. The gain should be of 100% when using these polymers. Note that this power loss was calculated in the active zone.

CONCLUSIONS

Using the V. K. Stokes micro-continuum theory for describing the flow of couple-stress lubricants consisting of base oil and VI improver additives, the couple stress effects on the dynamic behavior of the big end connecting rod bearings for both diesel and gasoline engines were investigated. A transient modified Reynolds equation was derived in order to take into consideration the effects of couple stresses resulting from the presence of polymer additives in the base oil. The mobility method was used to predict the crankpin center trajectories. From this study, the following conclusions may be drawn:

1. The couple stress effects (increasing the couple stress parameter) produce higher oil-film thickness and more contracted trajectories.
2. The maximum film pressure decreases with increasing couple stress parameter, as well as the side leakage flow.
3. A drastic decrease of power loss with increasing couple stress parameter is also observed.

ACKNOWLEDGEMENTS

The authors wish to thank the anonymous reviewers, whose comments have been of immense help in bringing the paper to its present form. The authors also wish to express their sincere thanks to Professor John A. Tichy of the Rensselaer Polytechnic Institute (USA) for reading previous versions of this paper and for suggesting many improvements.

REFERENCES

(1) Stokes, V. K. (1966), "Couple-Stresses in Fluids," *The Physics of Fluids*, **9**, pp 1709-1715.
(2) Ariman, T. T. and Sylvester, N. D. (1973), "Micro-Continuum Fluid Mechanics: A Review," *Int. Eng. Sci.*, **11**, pp 905-930.
(3) Ariman, T. T. and Sylvester, N. D. (1974), "Application of Micro-continuum," *Int. Eng. Sci.*, **11**, pp 905-930.
(4) Lin, J. R. (1998), "Squeeze Film Characteristics of Long Journal Bearings: Couple-Stress Fluid Model," *Tribology Int.*, **30**(1), pp 53-58.
(5) Lin, J. R. (1998), "Squeeze Film Characteristics of Finite Journal Bearings: Couple-Stress Fluid Model," *Tribology Int.*, **31**(4), pp 201-207.
(6) Lin, J. R. (1999), "Static and Dynamic Characteristics of Externally Pressurized Circular Step Thrust Bearings Lubricated with Couple-Stress Fluids," *Tribology Int.*, **32**(4), pp 207-216.
(7) Mokhiamer, U. M., Crosby, W. A. and El-Gamal, H. A. (1999), "A Study of a Journal Bearing Lubricated by Fluids with Couple-Stress Considering the Elasticity of the Liner," *Wear*, **224**, pp 194-201.
(8) Lahmar, M. (2005), "Elastohydrodynamic Analysis of Double-Layered Journal Bearings Lubricated with Couple-Stress Fluids," *Journal of Engineering Tribology, Proc. IMechE Part J*, **219**, pp 145-171.
(9) Wang, X. L., Zhu, K. Q. and Wen, S. Z. (2001), "Thermohydrodynamic Analysis of Journal Bearings Lubricated with Couple-Stress Fluids," *Tribology Int.*, **34**, pp 335-343.
(10) Wang, X. L., Zhu, K. Q. and Wen, S. Z. (2002), "On the Performance of Dynamically Loaded Journal Bearings Lubricated with Couple-Stress Fluids," *Tribology Int.*, **35**, pp 185-191.
(11) Booker, J. F. (1971), "Dynamically Loaded Journal Bearings: Numerical Application of the Mobility Method," *ASME Journal of Tribology, Ser. F*, pp 168-174.
(12) Vincent B., Maspeyrot P. and Frene J. (1996), "Cavitation in Dynamically Loaded Journal Bearings Using Mobility Method," *Wear*, **193**, pp 155-162.

(13) Christopherson, D. G. (1941), "A New Mathematical Method for the Solution of the Oil Film Lubrication Problems," *Proc. I. Mech. E.*,**146**, pp 126-135.

(14) Campbell, J., Love, P.P., Martin, F. A., and Rafique, S. O. (1967), "Bearings for Reciprocating Machinery: A Review of the Present State of the Theoretical, Experimental and Service Knowledge," *Proc. I. Mech. E* , London, **182**, Part 3A, pp 51-74.

(15) Martin, F. A. (1982), "Developments in Engine Bearings," *Proc. of the 9th Leeds-Lyon Symposium on Tribology.*

APPENDIX A

In thin-film theory, the dimension across the film thickness is small compared to the others. From this assumption, we can determine the order of magnitude for the different terms of Eq. [7]. Thus:

$$\tilde{x} = \frac{x}{L}, \quad \tilde{y} = \frac{y}{h}, \quad \tilde{z} = \frac{z}{L}, \quad \tilde{t} = \frac{tV}{L}, \quad \tilde{u} = \frac{u}{V}, \quad \tilde{v} = \frac{vL}{Vh},$$
$$\tilde{w} = \frac{w}{V}, \quad \tilde{\mu} = \frac{\mu}{\mu_0}, \quad \tilde{\rho} = \frac{\rho}{\rho_0}, \quad \text{and} \quad \tilde{\eta} = \frac{\eta}{\eta_0}$$

In these expressions, L and V represent, respectively, the characteristic dimension and speed according to (o,x) and (o,z) axes, h and Vh/L according to (o,y); while L/V gives the order of magnitude of time; and μ_0, η_0 are physical constants for the fluid. Using these dimensionless variables, we can set $\tilde{p} = p\frac{h^2}{VL\mu_0}$.

Thus, Eq. [7] reads:

$$\frac{\partial \tilde{p}}{\partial \tilde{x}} = -\varepsilon \Re_h \tilde{\rho} \frac{D\tilde{u}}{D\tilde{t}} + \tilde{\mu}\left[\varepsilon^2\left(\frac{\partial^2 \tilde{u}}{\partial \tilde{x}^2} + \frac{\partial^2 \tilde{u}}{\partial \tilde{z}^2}\right) + \frac{\partial^2 \tilde{u}}{\partial \tilde{y}^2}\right] - \left(\frac{\ell_0}{h}\right)^2 \tilde{\eta}\left[\varepsilon^4\left(\frac{\partial^4 \tilde{u}}{\partial \tilde{x}^4} + \frac{\partial^4 \tilde{u}}{\partial \tilde{z}^4}\right) + \frac{\partial^4 \tilde{u}}{\partial \tilde{y}^4}\right] - 2\left(\frac{\ell_0}{h}\right)^2 \tilde{\eta} \times \left[\varepsilon^4 \frac{\partial^4 \tilde{u}}{\partial \tilde{x}^2 \partial \tilde{z}^2} + \varepsilon^2\left(\frac{\partial^4 \tilde{u}}{\partial \tilde{x}^2 \partial \tilde{y}^2} + \frac{\partial^4 \tilde{u}}{\partial \tilde{y}^2 \partial \tilde{z}^2}\right)\right]\right\} \quad [A2]$$

$$\frac{\partial \tilde{p}}{\partial \tilde{y}} = \varepsilon^2\left\{ - \varepsilon \Re_h \tilde{\rho} \frac{D\tilde{v}}{D\tilde{t}} + \tilde{\mu}\left[\varepsilon^2\left(\frac{\partial^2 \tilde{v}}{\partial \tilde{x}^2} + \frac{\partial^2 \tilde{v}}{\partial \tilde{z}^2}\right) + \frac{\partial^2 \tilde{v}}{\partial \tilde{y}^2}\right] - \left(\frac{\ell_0}{h}\right)^2 \tilde{\eta}\left[\varepsilon^4\left(\frac{\partial^4 \tilde{v}}{\partial \tilde{x}^4} + \frac{\partial^4 \tilde{v}}{\partial \tilde{z}^4}\right) + \frac{\partial^4 \tilde{v}}{\partial \tilde{y}^4}\right] - 2\varepsilon^2\left(\frac{\ell_0}{h}\right)^2 \tilde{\eta}\left[\frac{\partial^4 \tilde{v}}{\partial \tilde{x}^2 \partial \tilde{y}^2} + \varepsilon^2 \frac{\partial^4 \tilde{v}}{\partial \tilde{x}^2 \partial \tilde{z}^2} + \frac{\partial^4 \tilde{v}}{\partial \tilde{y}^2 \partial \tilde{z}^2}\right]\right\} \quad [A3]$$

$$\frac{\partial \tilde{p}}{\partial \tilde{z}} = -\varepsilon \Re_h \tilde{\rho} \frac{D\tilde{w}}{D\tilde{t}} + \tilde{\mu}\left[\varepsilon^2\left(\frac{\partial^2 \tilde{w}}{\partial \tilde{x}^2} + \frac{\partial^2 \tilde{w}}{\partial \tilde{z}^2}\right) + \frac{\partial^2 \tilde{w}}{\partial \tilde{y}^2}\right] - \left(\frac{\ell_0}{h}\right)^2 \tilde{\eta}\left[\varepsilon^4\left(\frac{\partial^4 \tilde{w}}{\partial \tilde{x}^4} + \frac{\partial^4 \tilde{w}}{\partial \tilde{z}^4}\right) + \frac{\partial^4 \tilde{w}}{\partial \tilde{y}^4}\right] - 2\left(\frac{\ell_0}{h}\right)^2 \tilde{\eta}\left[\varepsilon^4 \frac{\partial^4 \tilde{w}}{\partial \tilde{x}^2 \partial \tilde{z}^2} + \varepsilon^2\left(\frac{\partial^4 \tilde{w}}{\partial \tilde{x}^2 \partial \tilde{y}^2} + \frac{\partial^4 \tilde{w}}{\partial \tilde{y}^2 \partial \tilde{z}^2}\right)\right] \quad [A4]$$

where $\Re_h = \rho_0 \frac{Vh}{\mu_0}$ is the local Reynolds number and $\varepsilon = \frac{h}{L}$ is a scale parameter of order 10^{-3}.

Neglecting the terms factor of ε^2 and ε^4 , it remains:

$$\begin{cases} \dfrac{\partial \tilde{p}}{\partial \tilde{x}} = -\varepsilon \tilde{\rho} \Re_h \dfrac{D\tilde{u}}{D\tilde{t}} + \tilde{\mu} \dfrac{\partial^2 \tilde{u}}{\partial \tilde{y}^2} - \tilde{\eta}\left(\dfrac{\ell_0}{h}\right)^2 \dfrac{\partial^4 \tilde{u}}{\partial \tilde{y}^4} \\ \dfrac{\partial \tilde{p}}{\partial \tilde{y}} = 0 \rightarrow \tilde{p} = \tilde{p}\,(\tilde{x}, \tilde{z}) \\ \dfrac{\partial \tilde{p}}{\partial \tilde{z}} = -\varepsilon \tilde{\rho} \Re_h \dfrac{D\tilde{w}}{D\tilde{t}} + \tilde{\mu} \dfrac{\partial^2 \tilde{w}}{\partial \tilde{y}^2} - \tilde{\eta}\left(\dfrac{\ell_0}{h}\right)^2 \dfrac{\partial^4 \tilde{w}}{\partial \tilde{y}^4} \end{cases} \quad [A5]$$

If $\varepsilon \Re_h \ll 1$, Eq. [A5] reduces to:

$$\begin{cases} \dfrac{\partial \tilde{p}}{\partial \tilde{x}} = \tilde{\mu} \dfrac{\partial^2 \tilde{u}}{\partial \tilde{y}^2} - \tilde{\eta}\left(\dfrac{\ell_0}{h}\right)^2 \dfrac{\partial^4 \tilde{u}}{\partial \tilde{y}^4} \\ \dfrac{\partial \tilde{p}}{\partial \tilde{y}} = 0 \\ \dfrac{\partial \tilde{p}}{\partial \tilde{z}} = \tilde{\mu} \dfrac{\partial^2 \tilde{w}}{\partial \tilde{y}^2} - \tilde{\eta}\left(\dfrac{\ell_0}{h}\right)^2 \dfrac{\partial^4 \tilde{w}}{\partial \tilde{y}^4} \end{cases} \quad [A6]$$